SEARCH FOR THE MSSM HIGGS BOSONS WITH THE CMS DETECTOR AT THE LHC*

Michał Szleper

on behalf of the CMS Collaboration

National Center for Nuclear Research
Hoża 69, 00-681 Warszawa, Poland

(Received April 30, 2013)

The CMS experiment carried out searches for the neutral and charged Higgs bosons of the Minimal Supersymmetric extension of the Standard Model based on data collected in 2011 at the center-of-mass energy of 7 TeV or a combination of 7 TeV and the first part of 8 TeV data taken in 2012. Results provide the most stringent MSSM limits in the $\tan\beta$ *versus* M_A plane to date, and severely constrain the allowed MSSM parameter space.

DOI:10.5506/APhysPolB.44.1603
PACS numbers: 14.80.Da

1. Introduction

The recent discovery of a Higgs-like boson at around 125 GeV at the LHC [1] was the final confirmation of the tremendous success of the Standard Model (SM) as a theory of elementary particles and fundamental interactions. However, there are good reasons to believe this is not the entire story. The SM Higgs boson suffers from quadratically divergent self-energy corrections at high energy. A number of solutions to the problem has been proposed, one of them being supersymmetry (SUSY), a symmetry relating the fundamental fermions and bosons, which provides cancellation of these divergences via additional contributions from the respective supersymmetric partners of all known particles. The MSSM is the simplest of this class of models.

Supersymmetry requires at least two Higgs doublets to provide couplings to up-type and down-type fermions, respectively. After electroweak symmetry breaking this leads to five physical Higgs particles: two neutral scalars,

* Presented at the Cracow Epiphany Conference on the Physics After the First Phase of the LHC, Kraków, Poland, January 7–9, 2013.

h and H, a neutral pseudoscalar, A, and a pair of charged Higgses, $H^{\pm}$. These minimal requirements define the expected Higgs sector content in the MSSM. The three neutral bosons are often collectively denoted as ϕ. At tree level, the MSSM Higgs sector can be described in terms of two parameters which are usually chosen to be $\tan\beta$, the ratio of the two vacuum expectation values, and M_A, the mass of the CP-odd Higgs. Higher order dependencies on the remaining MSSM parameters are usually taken into account by considering a number of fixed benchmark scenarios. Throughout this paper, the so-called $m_h^{\max}$ scenario will be assumed, which is known to yield rather conservative expected exclusion limits in the $\tan\beta$ *versus* M_A plane. The relations between various Higgs boson masses at different $\tan\beta$ values, within the MSSM $m_h^{\max}$ scenario, are shown in Fig. 1. For large $\tan\beta$, if $M_A < 130$ GeV, the masses of h and A are nearly degenerate. Conversely, if $M_A > 130$ GeV, then the masses of H and A are nearly degenerate. In particular, at least one boson is always expected below 135 GeV, consistently with the recent LHC discovery. It was noted that interpretation of the LHC Higgs-like boson as the h boson of the MSSM translates into a constraint on the allowed $\tan\beta$ *versus* M_A parameter space, affecting mainly the region of large M_A and $\tan\beta > 10$ [2].

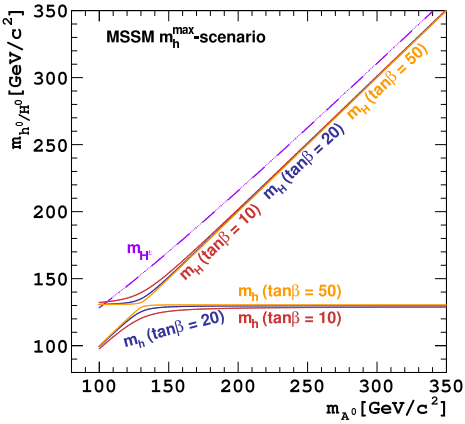

Fig. 1. The Higgs bosons masses in the MSSM $m_h^{\max}$ scenario.

Neutral MSSM Higgs production at the LHC, $pp \to \phi + X$, is dominated by two processes: $b\bar{b}$-associated production and gluon–gluon fusion via top (and bottom) loops. For large $\tan\beta$ values, the Higgs couplings to down-type and third generation fermions are enhanced with respect to the SM. The $b\bar{b}$-associated production dominates for sufficiently large $\tan\beta$, while gluon–gluon fusion dominates for moderate $\tan\beta$. At all masses, ϕ decays into third generation fermions are enhanced compared to the SM Higgs. Three different decay modes have been considered in CMS: $\phi \to b\bar{b}$, with a

high (∼90%) branching fraction, but burdened by large QCD background, $\phi \to \tau^+\tau^-$, including both hadronic and leptonic τ decays, and $\phi \to \mu^+\mu^-$, with the cleanest signature, but low yield.

A charged Higgs boson at the LHC can manifest itself as an alteration of the τ yield in top pair decays compared to the SM. If the mass of the $H^\pm$ is smaller than the difference between the top mass and the bottom mass, the top quark can decay via $t \to H^+b$ (and charge conjugate) and such decays may be detectable in $t\bar{t}$ pair production. For $\tan\beta > 5$, the charged Higgs decays preferably into a τ lepton and a neutrino. Four different final states have been considered in CMS, accordingly to some of the possible subsequent decay modes of the τ and the W: τ_{had}+jets (where τ_{had} denotes a tau lepton decaying into hadrons), $\tau_{\text{had}} + e/\mu$ and $e + \mu$.

2. The CMS experiment

A detailed description of the CMS detector can be found elsewhere [3]. The central feature of the CMS apparatus is a superconducting solenoid providing a magnetic field of 3.8 T. Within the field volume there are the silicon pixel and strip tracker, the crystal electromagnetic calorimeter (ECAL) and the brass/scintillator hadron calorimeter (HCAL). The solenoid allows tracks with transverse momentum (p_{T}) as low as 100 MeV to be reconstructed and the tracker provides a p_{T} resolution of 1% at 100 GeV. The energy resolution achieved by ECAL is $3\%/\sqrt{E_{\text{T/GeV}}}$ while in HCAL it is $100\%/\sqrt{E_{\text{T/GeV}}}$. Muons are measured in gas-ionization detectors embedded in the steel return yoke.

To combine information from all CMS subdetectors in order to identify and reconstruct individual particles in the event, namely muons, electrons, photons and charged and neutral hadrons, a particle-flow algorithm is used [4]. From the resulting particle list, jets, hadronically decaying taus and missing transverse energy (MET, defined as the magnitude of the vector sum of all the transverse momenta), are also reconstructed. Jets are reconstructed using the anti-k_{T} jet algorithm [5] with a distance parameter $R = 0.5$. Hadronically decaying taus are reconstructed using the Hadron Plus Strips (HPS) algorithm [6], which considers candidates with one charged pion and up to two neutral pions or three charged pions. To tag jets coming from b-quark decays, the Combined Secondary Vertex (CSV) algorithm is used [7]. This algorithm is based on the reconstruction of secondary vertices, together with track-based lifetime information.

An average of 10 (20) proton–proton interactions occurred per LHC bunch crossing in 2011 (2012), making the reconstruction of physics objects challenging. For each reconstructed collision vertex, the sum of the p_{T}^2 of all the tracks associated to the vertex is computed and the one with the

highest value is taken as the primary collision vertex. In order to mitigate the effect of multiple overlapping interactions on the reconstruction of jets and MET, dedicated algorithms that filter all components not originating from the primary interaction are used.

3. Search for the neutral MSSM Higgs bosons in the $\tau^+\tau^-$ decay mode

The study presented here was carried out using 4.9 fb^{-1} of CMS data collected at the center-of-mass energy of 7 TeV (2011) and 12.1 fb^{-1} of data at 8 TeV (2012). A detailed description of this analysis can be found in Ref. [8].

Four final states were considered: $e+\tau_{\mathrm{had}}$, $\mu+\tau_{\mathrm{had}}$, $e+\mu$ and $\mu^+\mu^-$. Online trigger selection required a combination of either electron, muon and tau trigger objects. The identification criteria and p_{T} thresholds of these objects were progressively tightened as the LHC instantaneous luminosity increased over time. Offline, events were selected with two isolated opposite-charge leptons, including electrons of $p_{\mathrm{T}} > 20$ GeV (24 GeV) and pseudorapidity $|\eta| < 2.1$, muons with $p_{\mathrm{T}} > 20$ GeV (24 GeV) and $|\eta| < 2.1$, and hadronic taus with $p_{\mathrm{T}} > 20$ GeV and $|\eta| < 2.3$, in the 2011 (2012) datasets, respectively. Electrons with $|\eta| < 2.3$ were used in the $e + \mu$ mode. Events with additional isolated leptons with $p_{\mathrm{T}} > 15$ GeV were rejected. MET of at least 25 GeV was required in the $e + \tau_{\mathrm{had}}$ mode.

Additional selection criteria were imposed to suppress the background from W + jets with a jet misidentified as hadronic tau. In the $e + \tau_{\mathrm{had}}$ and $\mu + \tau_{\mathrm{had}}$ modes, this was achieved by placing a cut on the transverse mass of the electron or muon and MET, $M_{\mathrm{T}} < 40$ GeV. In the $e + \mu$ and $\mu^+\mu^-$ modes, a topological cut was applied that exploits the difference in the angular distributions between tau and W leptonic decays. This was done by considering the ζ axis defined as the bisector of the directions of the visible leptons transverse to the beam direction. We further define P_ζ^{vis} and P_ζ^{miss} as the projections of the visible lepton and of the MET, onto ζ, respectively. The present analysis required $P_\zeta^{\mathrm{miss}} - 0.85\, P_\zeta^{\mathrm{vis}} > -25$ GeV.

To enhance the sensitivity to the two main Higgs production mechanisms, events were further split into two mutually exclusive categories: in the B-Tag category, we required at least one additional b-tagged jet with $p_{\mathrm{T}} > 20$ GeV and not more than one jet with $p_{\mathrm{T}} > 30$ GeV; in the No B-Tag category, events were required to have no b-tagged jets with $p_{\mathrm{T}} > 20$ GeV.

The largest background originates from $Z \to \tau\tau$ and was estimated using the technique called "embedding". Here, a $Z \to \mu\mu$ data sample was selected and the muons were replaced with simulated tau decay products. The normalization is determined from the observed yield of $Z \to \mu\mu$ events.

Another important source of background are QCD multijet events with one jet misidentified as an isolated electron or muon and another jet misidentified as a τ_{had}. These were estimated using the yield of same-sign $\tau^{\pm}\tau^{\pm}$ events in the data. The remaining W + jets background is estimated from events with large M_{T} with the overall shape deduced from simulation (hadronic modes) or from data with relaxed lepton isolation criteria on one lepton (leptonic modes). The shape of the $t\bar{t}$ and diboson backgrounds is taken from simulation and the event yields were determined from measurements in background enriched regions.

The invariant mass of the tau pair was reconstructed from a kinematic fit based on the maximum likelihood technique. The algorithm computes the mass value that is the most probable given the visible decay product kinematics. It reproduces the true value of the tau pair mass with an uncertainty of 15–20%. The observed tau pair mass distributions in each mode are shown in Figs. 2 and 3 for the two event categories, respectively. Also

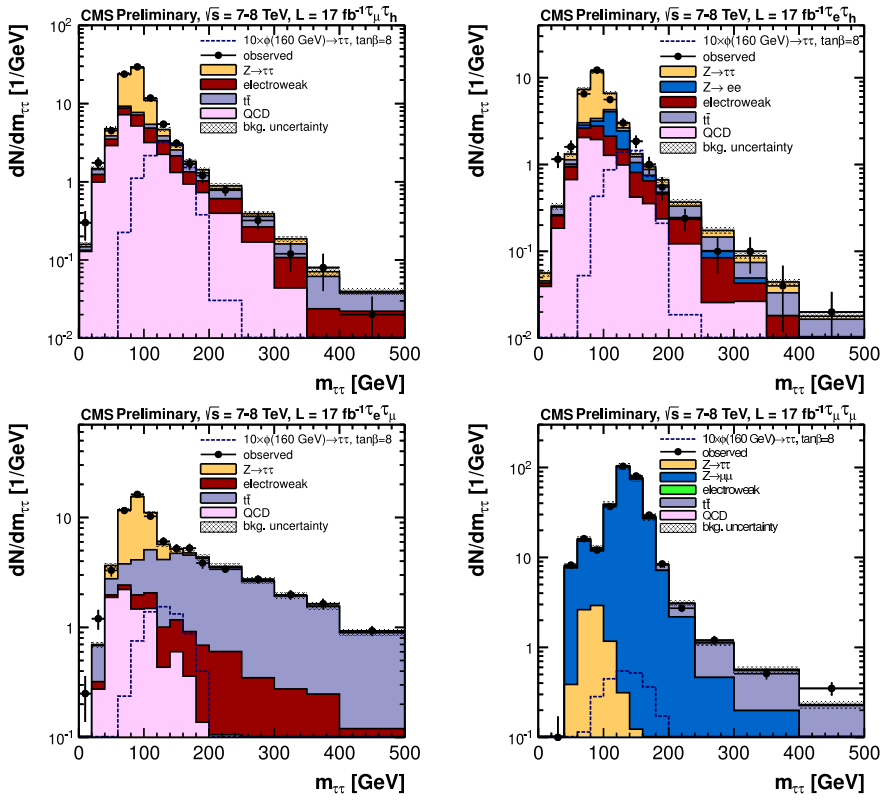

Fig. 2. The $\tau\tau$ invariant mass distributions in the B-Tag category and for the four final states: $\mu\tau_{\mathrm{had}}$ (upper left), $e\tau_{\mathrm{had}}$ (upper right), $e\mu$ (lower left) and $\mu\mu$ (lower right). Shown are data points and the estimated backgrounds.

shown are the predicted SM background yields and examples of a hypothetical $\phi \to \tau\tau$ signal. The ϕ production cross sections were provided by the LHC Higgs Cross Section Group [9]. Signal contributions from h, H and A and the two production mechanisms were considered. No significant excess over the background has been observed.

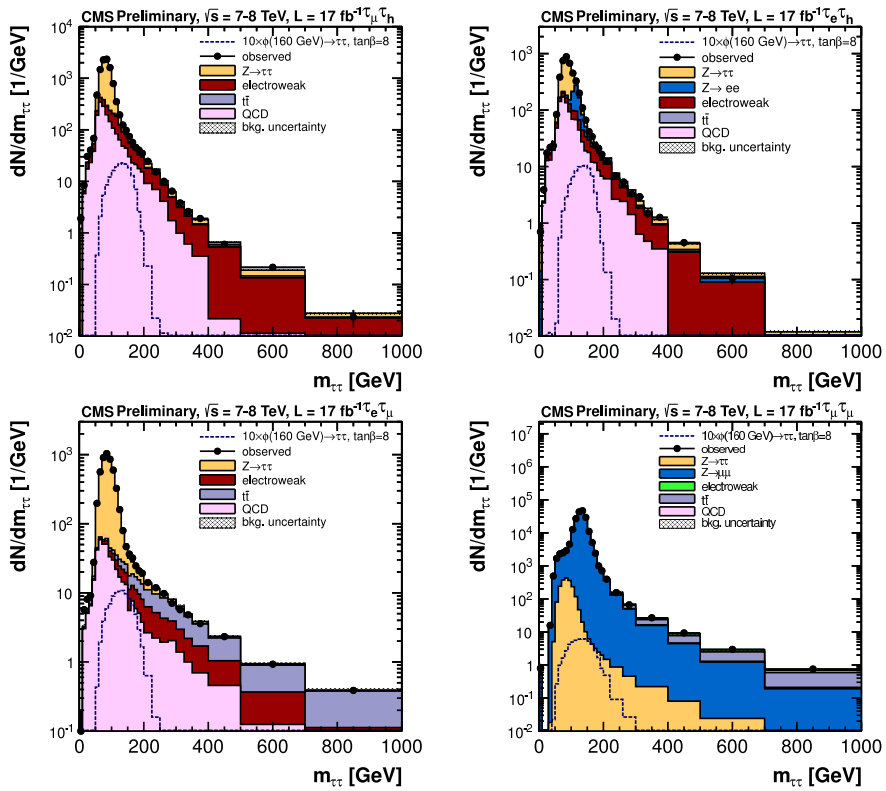

Fig. 3. The $\tau\tau$ invariant mass distributions in the No B-Tag category and for the four final states: $\mu\tau_{\rm had}$ (upper left), $e\tau_{\rm had}$ (upper right), $e\mu$ (lower left) and $\mu\mu$ (lower right). Shown are data points and the estimated backgrounds.

The final result comes from a binned maximum likelihood fit performed simultaneously for the four final states with two categories each. Taken into account were systematic uncertainties arising from the total luminosity, jet energy scale, backgrounds, lepton ID and isolation efficiency, trigger efficiency and b-tagging. Figure 4 shows the resulting 95% C.L. exclusion limit in the tanβ *versus* M_A plane calculated within the $m_h^{\rm max}$ scenario. The exclusion limits from LEP experiments [10] are also shown. This result extends the previously explored range [11] to larger values of M_A and excludes values of tanβ as low as 5 for any $M_A < 250$ GeV.

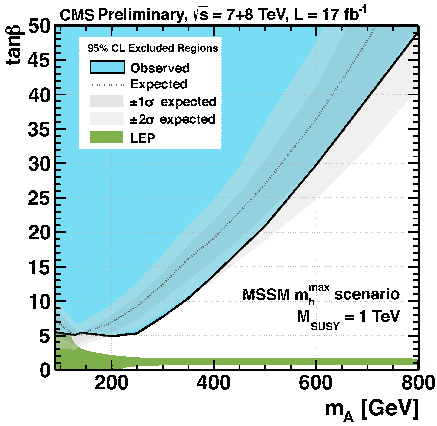

Fig. 4. Observed and expected 95% C.L. exclusion limits in the MSSM plane $M_A - \tan\beta$ from the search of $\phi \to \tau^+\tau^-$. Also shown are LEP limits.

4. Search for the neutral MSSM Higgs bosons in the $b\bar{b}$ decay mode

Results presented here correspond to a total luminosity of 2.7–4.8 fb^{-1} of data collected during 2011 at 7 TeV. The signal was searched for in final states characterized either purely by jets ("all-hadronic") or with an additional non-isolated muon ("semi-leptonic"). Details of the respective analyses can be found in Ref. [12]. Each signature is selected by specialized triggers that exploit the online algorithms for the identification of b quark jets. The search strategy is to look for an enhancement in the invariant mass distribution of the two leading b-jets in the sample of events with at least 3 b-jets. Both analyses are sensitive to the $b\bar{b}$-associated Higgs production mechanism.

Required offline in the "all-hadronic" mode were at least 3 b-tagged jets with $|\eta| < 2.2$ and the two leading ones separated by at least $\Delta R = \sqrt{\Delta\eta^2 + \Delta\varphi^2} > 1$ in order to suppress background from gluon splitting into b pairs. In the "semi-leptonic" category, only two leading jets were required to be b-tagged, while the third jet must pass a looser tagging criterion. Jets must have $|\eta| < 2.6$, their separation $\Delta R > 1$ and, in addition, a muon with $p_{\mathrm{T}} > 15$ GeV is required. The muon must be used in the reconstruction of one of the jets. As the jet p_{T} thresholds had to be increased during the run to handle the LHC increasing luminosity, two separate analyses were done for each category, corresponding to lower and higher thresholds. The former extends our sensitivity to lower ϕ masses, namely $M_\phi < 180$ GeV, and corresponds to a data sample of 2.7 fb^{-1}. The latter corresponds to the full 7 TeV sample, but is mainly sensitive to the medium- and high-mass scenario, $M_\phi \geq 180$ GeV.

Background is completely dominated by QCD multijet events. In the "all-hadronic" signature background is modeled with a combination of templates derived from a sample of double b-tag events, *i.e.*, with the b-tagging requirement relaxed on one jet. Templates are distributions in a two-dimensional space spanned by the mass of the two leading jets, $M_{1,2}$, and EventBTag, a unique variable that combines the b-tagging information of the three jets into a single number. Each template represents a different assumed true flavor of the untagged jet and is obtained by scaling the distribution with the appropriate b-tagging probability for this flavor. Those probabilities were computed from simulation as a function of jet p_{T} and η and corrected with data wherever appropriate. The signal is extracted by fitting a linear combination of signal and background templates to the observed data histogram in the $M_{1,2}$ and EventBTag space. One-dimensional projections onto $M_{1,2}$ of the fits for the two mass scenarios, with the contributions from the different background templates and an example of a signal template, are shown in Fig. 5.

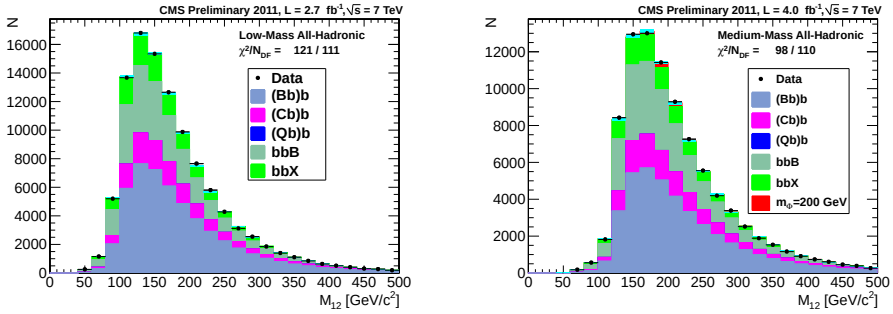

Fig. 5. The di-jet invariant mass from the selected events in the "all-hadronic" category and for the two mass scenarios.

Two independent data-driven background estimation methods were developed for the "semi-leptonic" signature. One exploits the double b-tag sample (B-tag Matrix method), the other one uses single b-tag events ("Hyperball method") and is based on calculating the probability of a given event to appear signal-like as a function of several input variables characterizing the jets and the event. Because both methods use exclusive data samples, the final background estimation comes from combining their results. Signal extraction is done via a maximum likelihood fit to the $M_{1,2}$ distribution in the data. Fit results for the two mass scenarios are shown in Fig. 6.

As no evidence of signal is found in any of the above analyses, the results were combined and translated into exclusion limits. Figure 7 shows the 95% C.L. exclusion limit on the cross section for $b\bar{b}$-associated MSSM Higgs production in pp collisions at 7 TeV (left) and an exclusion limit in the $\tan\beta$ *versus* M_A plane from this channel (right).

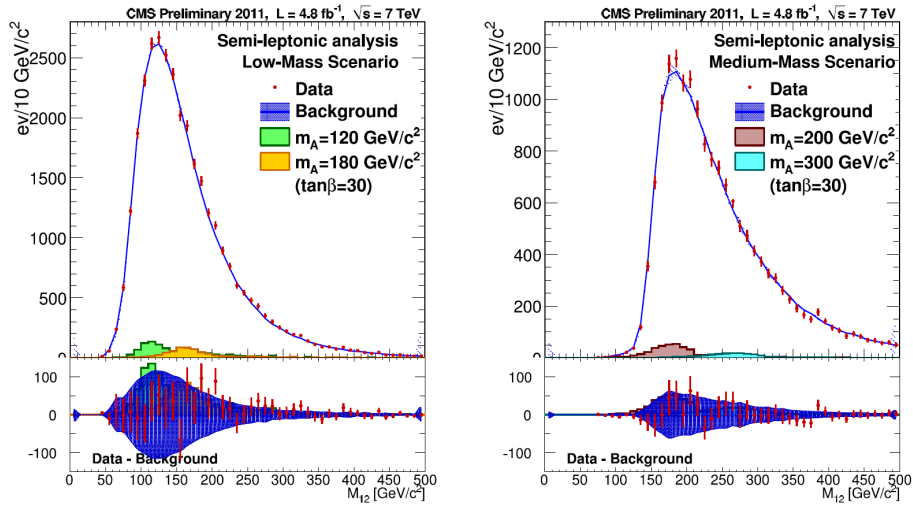

Fig. 6. The di-jet invariant mass from the selected events in the "semi-leptonic" category and for the two mass scenarios.

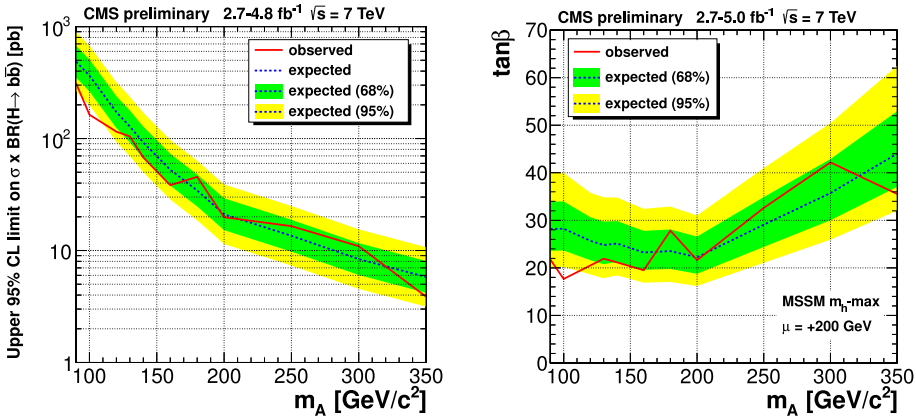

Fig. 7. Left: Observed and expected upper limits for the cross section times branching ratio at 95% C.L. from a search of $\phi \to b\bar{b}$ — results of the all-hadronic and semi-leptonic analyses, as well as the two mass scenarios, combined. Right: Observed and expected upper limits at 95% C.L. in the MSSM plane $(\tan\beta, M_A)$.

5. Search for the neutral MSSM Higgs bosons in the $\mu^+\mu^-$ decay mode

Data for this study were recorded in 2011 at a center-of-mass energy of 7 TeV and correspond to an integrated luminosity of 4.96 fb^{-1}. The

signature of the sought process is the presence of two isolated, oppositely charged muons with high p_{T}. Data were collected using an unprescaled single muon trigger. Details of this analysis can be found in Ref. [13].

The search is sensitive to both the $b\bar{b}$-associated ϕ production and the gluon fusion processes. Offline, the muons were required to have $|\eta| < 2.1$, their respective p_{T} thresholds were 30 and 20 GeV and MET was required to be below 30 GeV. Additionally, events were categorized into three classes. In Category 1, an extra b-tagged jet with $p_{\mathrm{T}} > 20$ GeV and $|\eta| < 2.4$ was required, separated from any muon by $\Delta R > 0.5$. In Category 2, a third low-p_{T} muon at $|\eta| < 2.4$ and separated by $\Delta R > 0.5$ from any of the first two muons was required. Events that did not belong to Category 1 or Category 2 were assigned to Category 3.

Most of the background comes from the Drell–Yan $Z \to \mu^+\mu^-$ process. Also important sources of background are $t\bar{t}$ production for Category 1 and W^+W^- production for Category 3. The sum of the di-muon invariant masses from the three categories is shown in Fig. 8 (left), both for data and simulated backgrounds. However, the final result was extracted following a fully data-driven approach, by fitting to the data an analytical function that includes contributions from the background described in terms of a Breit–Wigner distribution plus a photon exchange term proportional to $1/M^2_{\mu\mu}$, and contributions from the signal which are a linear combination of three Breit–Wigners, one for each Higgs boson, taking into account its experimental resolution.

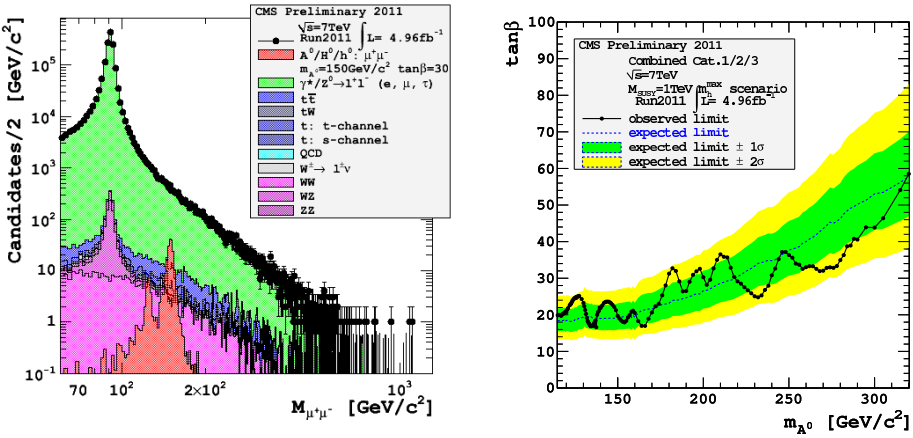

Fig. 8. Left: The di-muon invariant mass distribution from data and background estimation — from a search of $\phi \to \mu^+\mu^-$ — sum of all event categories. Right: Observed and expected upper limits at 95% C.L. in the MSSM plane $(\tan\beta, M_A)$.

No evidence for an excess over the predicted background is found. The resulting 95% C.L. limit on MSSM Higgs production times the branching fraction for $\phi \to \mu^+\mu^-$ ranges from 40–20 fb for M_A between 150–300 GeV. 95% C.L. exclusion limits in the tanβ *versus* M_A plane from this channel are shown in Fig. 8 (right).

6. Search for the charged MSSM Higgs boson

This search corresponds to about 2 fb^{-1} of data collected by CMS in 2011 at a center-of-mass energy of 7 TeV. Four final states were studied: $\tau_{\rm had}$ + jets, $\tau_{\rm had} + e/\mu$ and $e + \mu$, all requiring missing transverse energy and multiple jets. Details of this analysis can be found in Ref. [14].

The $\tau_{\rm had}$ + jets sample was collected with a trigger requiring a hadronic tau and MET. Offline analysis required additionally at least three jets with $p_{\rm T} > 30$ GeV, at least one of them b-tagged, and a reconstructed $\tau_{\rm had}$ with $p_{\rm T} > 40$ GeV and $|\eta| < 2.1$. In order to suppress the multijet background, MET > 50 GeV was required and the azimuthal angle separation between the tau and the MET vector, $\Delta\varphi < 160°$. Moreover, to reduce the amount of taus from W decays, only 1-track taus were selected and the momentum ratio of the track to the tau was required to be $p^{\rm trk}/p^{\tau_{\rm had}} > 0.7$, to exploit the different polarizations of taus originating from $H^\pm$ or $W^\pm$ decays.

The $\tau_{\rm had} + e/\mu$ samples were collected using triggers that selected events with an electron and two jets, or a muon, respectively. Electrons with $p_{\rm T} > 35$ GeV and $|\eta| < 2.5$, muons $p_{\rm T} > 30$ GeV and $|\eta| < 2.1$, and taus with $p_{\rm T} > 20$ GeV and $|\eta| < 2.4$ were selected. Events were also required to have at least two high-$p_{\rm T}$ jets, including at least one b-tagged. Finally, MET was required to be > 45 GeV (40 GeV) for $\tau_{\rm had} + e(\mu)$.

The $e + \mu$ sample was collected with a dedicated electron + muon trigger path. The minimum transverse momentum for both leptons was $p_{\rm T} > 20$ GeV, $|\eta| < 2.5$ for electrons and $|\eta| < 2.4$ for muons. In addition, at least two high-$p_{\rm T}$ jets were required and at least one b-tagged.

Wherever applicable, opposite-charge leptons were required ($\tau_{\rm had} + e/\mu$, $e + \mu$) and isolation criteria imposed. Events with additional isolated electrons or muons were rejected.

The main background in the $\tau_{\rm had}$ + jets channel are QCD mulitjet events with jets that mimic hadronic tau decays. It was estimated from data events that pass all the selection criteria except the τ-id and applying a weight equal to the fake rate of jet misidentification as τ, measured in a control region. Other backgrounds include W + jets, Z + jets, diboson production, as well as $t\bar{t}$. These were obtained using a control data sample defined with the same jet selection criteria as for $\tau_{\rm had}$ + jets, but with a muon instead of a $\tau_{\rm had}$. The transverse mass, $M_{\rm T}$, distribution shape was then obtained by "embedding",

i.e., replacing the muon with a simulated τ_{had} decay. The contribution from electroweak processes without τ production, but with a jet misidentified as a τ_{had} was estimated from simulation.

The dominant contributions to the background in the $\tau_{\text{had}} + e/\mu$ channel comes from W + jets and $t\bar{t}$ events with a jet misidentified as a τ_{had} and were estimated by calculating the probability of a fake tau reconstruction based on W + jet and multijet events. Other backgrounds, with a genuine τ_{had}, were estimated from simulation.

Backgrounds for the $e + \mu$ channel were estimated from simulation.

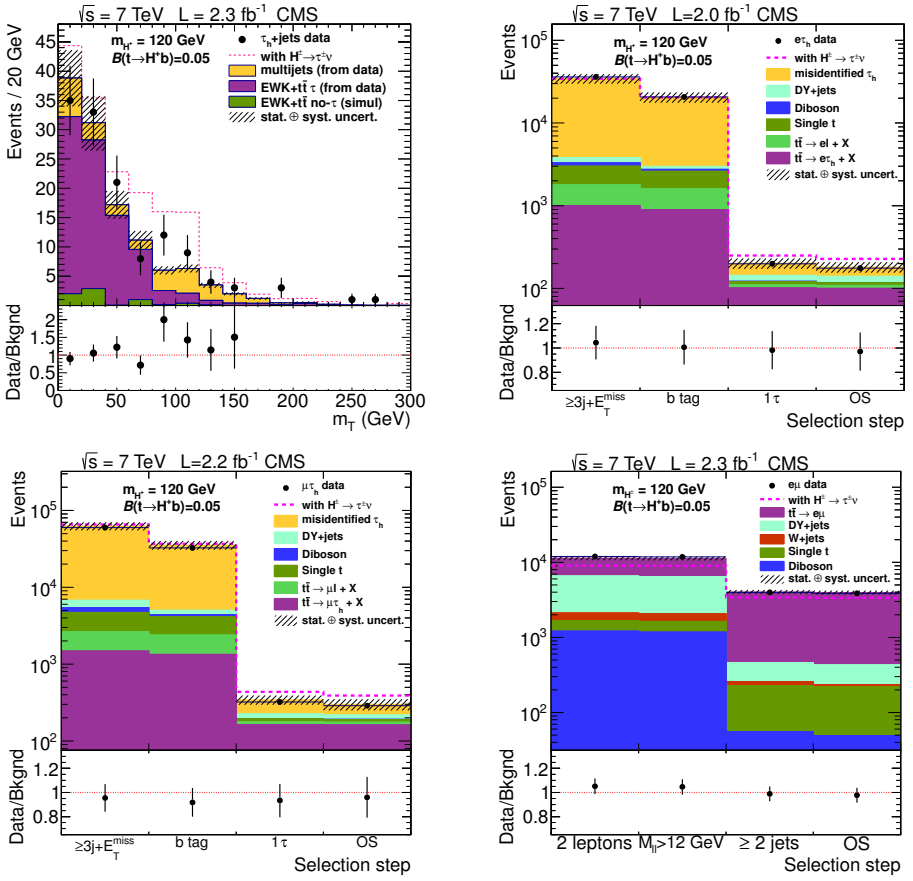

Fig. 9. Results of the search for the MSSM decay $H^{\pm} \to \tau^{\pm}\nu$ in the four final states: τ_{had} + jets (upper left), $e\tau_{\text{had}}$ (upper right), $\mu\tau_{\text{had}}$ (lower left) and $e\mu$ (lower right). Shown are data points and the estimated backgrounds. The τ_{had} + jets plot shows the transverse mass distributions, the other three plots show the event yields after each selection step.

Signal extraction comes from a binned maximum likelihood fit to the measured M_{T} distribution for the $\tau_{\mathrm{had}}+\mathrm{jets}$ channel and is based on simple event counting for the other channels. The results are given in Fig. 9.

For the $\tau_{\mathrm{had}}+\mathrm{jets}$ channel the M_{T} distribution from data and predicted background is shown, along with an example of simulated $H^{\pm}$ signal; for the other channels, event yields are shown after each selection step. The agreement between data points and predicted SM background is very good.

The results translate into a significant upper limit on the branching fraction of a top quark decaying into a charged Higgs, shown in Fig. 10 (left). At 95% C.L., $\mathrm{Br}(t \to H^{\pm}b) < 2$–$4\%$ with the $H^{\pm}$ mass ranging from 80 to 160 GeV. The corresponding 95% C.L. limits in the $\tan\beta$ *versus* $M_{H^{\pm}}$ are shown in Fig. 10 (right).

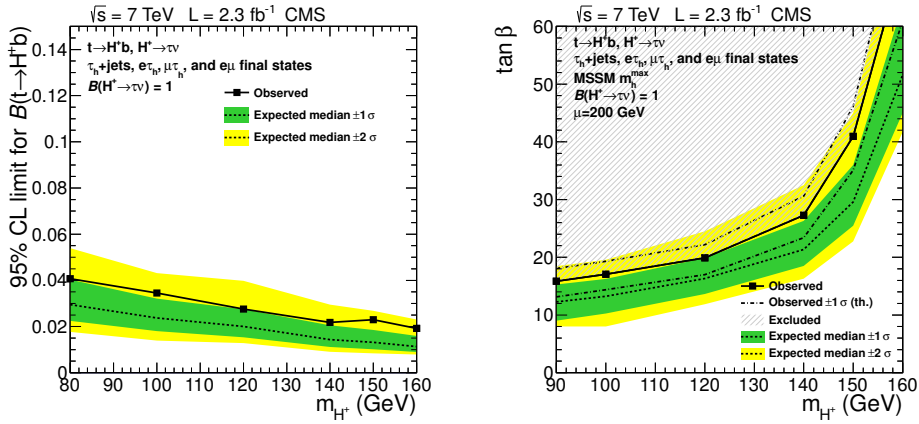

Fig. 10. Left: Observed and expected upper limits on the branching fraction of the top quark decay into the MSSM charged Higgs — all final states combined. Right: Observed and expected upper limits at 95% C.L. in the MSSM plane $(\tan\beta, M_{H^{\pm}})$.

7. Conclusions and outlook

We find no evidence for the MSSM nature of the Higgs boson.

Searches for the neutral MSSM Higgs bosons (h, H, A) were carried in three independent decay modes. In the most sensitive $\tau^{+}\tau^{-}$ decay mode, we have presented new results that come from a combined analysis of the 2011 7 TeV data and first part of the 2012 8 TeV data, corresponding to a total integrated luminosity of 17 fb^{-1}. We place new improved limits, the most stringent to date, in the MSSM $\tan\beta$ *versus* M_A parameter space. At a 95% C.L., we exclude a region reaching as low as $\tan\beta = 5$ for any $M_A < 250$ GeV.

Independent confirmation of parts of the above exclusion limits are obtained from searches in the $b\bar{b}$ and $\mu^+\mu^-$ decay channels, each based on 5 fb^{-1} of data collected by CMS at 7 TeV. Out of the former, a new stringent limit on the cross section for $b\bar{b}$ associated MSSM Higgs production is derived.

A search for the charged MSSM Higgs boson, $H^{\pm}$, based on 2–2.3 fb^{-1} of data collected at 7 TeV, likewise finds no evidence for signal and places a new, significant limit on the branching fraction $\mathrm{Br}(t \to H^{\pm}b) < 2$–$4\%$.

Taking into account that discovery of a Higgs-like boson at about 125 GeV also restricts the portion of the MSSM parameter space for it to be accommodated, the MSSM seems now rather severely constrained, albeit not entirely ruled out.

More 8 TeV data from 2012 is currently under analysis at CMS, so some of the shown limits may still be improved in the near future (or evidence for signal may be found).

REFERENCES

[1] CMS Collaboration, *Phys. Lett.* **B716**, 30 (2012); ATLAS Collaboration, *Phys. Lett.* **B716**, 1 (2012).

[2] S. Heinemeyer, O. Stal, G. Weiglein, *Phys. Lett.* **B710**, 201 (2012).

[3] CMS Collaboration, *JINST* **3**, S08004 (2008).

[4] CMS Collaboration, CMS Physics Analysis Summary CMS-PAS-PFT-09-001, 2009.

[5] M. Cacciari, G.P. Salam, G. Soyez, `arXiv:hep-ph/1111.6097`; *Phys. Lett.* **B641**, 57 (2006).

[6] CMS Collaboration, *JINST* **7**, P01001 (2012).

[7] CMS Collaboration, CMS Physics Analysis Summary CMS-PAS-BTV-11-004, 2012.

[8] CMS Collaboration, CMS Physics Analysis Summary CMS-PAS-HIG-12-050, 2012.

[9] LHC Higgs Cross Section Group, CERN Report CERN-2011-002, 2011.

[10] LEP Collaborations (ALEPH, DELPHI, L3, OPAL and the LEP Working Group), *Eur. Phys. J.* **C47**, 547 (2006).

[11] CDF and DØ collaborations, `arXiv:hep-ex/1003.3363`; CMS Collaboration, *Phys. Rev. Lett.* **106**, 231801 (2011); ATLAS Collaboration, *Phys. Lett.* **B705**, 174 (2011).

[12] CMS Collaboration, CMS Physics Analysis Summary CMS-PAS-HIG-12-033 and CMS-PAS-HIG-12-026, 2012; CMS Physics Analysis Summary CMS-PAS-HIG-12-027, 2012.

[13] CMS Collaboration, CMS Physics Analysis Summary CMS-PAS-HIG-12-011, 2012.

[14] CMS Collaboration, *J. High Energy Phys.* **1207**, 143 (2012).